2022-12

Reconstruction of provenance and tectonic setting of the Middle Jurrasic Yan'an Formation (Ordos Basin, North China) by analysis of major, trace and rare earth elements in the coals

Gao, J

10.1016/j.oregeorev.2022.105218
Ore Geology Reviews
Elsevier BV

Ore Geology Reviews 151 (2022) 105218

Contents lists available at ScienceDirect

Ore Geology Reviews

journal homepage: www.elsevier.com/locate/oregeorev

Reconstruction of provenance and tectonic setting of the Middle Jurrasic Yan'an Formation (Ordos Basin, North China) by analysis of major, trace and rare earth elements in the coals

Jie Gao [a], Dawei Lv [a,b], A.J. Tom van Loon [a], James C. Hower [c], Munira Raji [d], Yi Yang [a], Zhonghe Ren [a], Yujia Wang [a], Zhihui Zhang [a,*]

[a] College of Earth Science and Engineering, Shandong University of Science and Technology, Qingdao, China
[b] Laboratory for Marine Mineral Resources, Qingdao National Laboratory for Marine Science and Technology, Qingdao 266071, China
[c] University of Kentucky, Center for Applied Energy Research, 2540 Research Park Drive, Lexington, KY 40511, USA
[d] Sustainable Earth Institute, University of Plymouth, Devon PL4 8AA, UK

ARTICLE INFO

Keywords:
Ordos Basin
Yan'an Formation
Coal Geochemistry
Provenance analysis

ABSTRACT

The Middle Jurassic Yan'an Formation in the Ordos Basin (North China) is an important coal-bearing succession. Twenty coal samples and four samples of silty mudstones were collected from Coal Seam 2 of the Yan'an Formation in order to determine major, trace and rare earth elements; moreover, the geochemistry of the rare earth elements, and in particular yttrium, was investigated. The major elements investigation reveals that Si, Al, Na, K, and Ti are primarily found in clay minerals. Calcium is primarily found in calcite and iron is largely controlled by sulfur. The average REE (rare earth element) contents in the coals and silty mudstones are 15.17 μg/g and 210.57 μg/g, respectively. The Upper Continental Crust-normalized distribution patterns of the REE in the coals and silty mudstones show no obvious fractionation; however, they show negative Eu anomalies and negligible Ce anomalies. Correlations between the REE and the major elements indicate that the REE in the coals and silty mudstones are both derived from eroded rocks in the hinterland and mainly controlled by the presence of detrital minerals. We investigated some diagrams of major element, trace element, and REE from the coal seam to comprehend its provenance and tectonic setting. The findings indicate that they are mainly derived from felsic and intermediate rocks in a continental island arc setting. The REE analysis shows that various provenance areas supplied clastics when coal developed in the Yan'an Formation. The findings imply that provenance analysis should be taken into account when studying the sedimentary environments of coal-bearing successions.

1. Introduction

Analyses of the sedimentary environment of coal-bearing successions have been found to profit from the analysis of rare earth elements (REE) in both the coals themselves and the clastic sediments in between (Bhattacharjee et al., 2018; Zhao et al., 2019; Tatar and Alipour-Asll, 2020). Moreover, they provide insight into the post-depositional history of coal deposits because of their coherent behavior during different geochemical processes and their predictable fractionation patterns (Bau et al., 2014; Dai et al., 2016). This is because their mobility and controlling factors reflect certain geological and physical–chemical properties (Van der Weijden and Van der Weijden, 1995). Numerous geochemical studies of REE related to coal, mudstone, black shale, volcanic rock, and metal ores thus elucidated their provenance, tectonic setting, paleo-environment and other conditions related to their deposition (Piper, 1974; Eskenazy, 1987; Schatzel and Stewart, 2003; Qi et al., 2007; Dai et al., 2013, 2015; Arbuzov et al., 2019).

Analysis of rare earth elements, and particularly of yttrium, is also of economic interest because they play an ever more important role in the world economy of the 21st century (Kato et al., 2011; Balaram, 2019; Dushyantha et al., 2020). Although the primary sources of REE are carbonatites, alkaline igneous systems, ion-adsorbing clay deposits, and monazite/xenotime-bearing placer deposits (USGS (United States Geological Survey), 2021), coal deposits have become an important alternative source for REE (Seredin and Dai, 2012; Hower et al., 2015, 2016; Dai et al., 2016). REE are, however, not the only interesting

* Corresponding author.
E-mail address: zhzhihui@sdust.edu.cn (Z. Zhang).

https://doi.org/10.1016/j.oregeorev.2022.105218
Received 14 September 2022; Received in revised form 9 November 2022; Accepted 21 November 2022
Available online 22 November 2022

parameter that gives insight into the characteristics of the coal, the responsible processes and the various conditions of their setting. The source areas of the coal can be traced on the basis of the lithology, mineralogy and geochemistry of the clastic components, and this implies that also in this context the analysis of evenly distributed REE in the coal is important (Van der Flier-Keller, 1993). Local and temporal changes in REE are related to the nature of the parent rock and the tectonic background of the provenance area as shown in numerous studies (e.g., Piper, 1974; Eskenazy, 1987; Van der Flier-Keller, 1993; Dai et al., 2013; Bai et al., 2015).

The Ordos Basin was one of the world's largest continental basins during the Jurassic. Numerous coal beds dating from the early Middle Jurassic occur in the Yan'an Formation (Johnson et al., 1989; Wang et al., 2012; Wang et al., 2018; Zhang et al., 2021). The depositional environments of this formation have been studied extensively (Johnson et al., 1989; Guo et al., 2018; Zhang et al., 2021; Wang et al., 2012; Lei et al., 2017). Moreover, several studies have investigated the distribution of these coals (Wang et al., 2012), their sequence stratigraphy (Wang et al., 2012; Lv et al., 2020), and climatic circumstances (Tanner et al., 2012; Lei et al., 2017). Studies dealing with provenance and tectonic setting of these coals are fairly rare, however. We fill this gap in knowledge here by analyzing the inorganic geochemical characteristics of these coals on the basis of the occurrence patterns of major, trace and rare earth elements, and by tracing the provenance areas, and reconstructing the tectonic setting.

2. Geological setting

The Ordos Basin is located on the western margin of the North China Plate, covering an area of about 250,000 km^2 (Wang et al., 2014) (Fig. 1A). It is the second largest continental basin in China (Ao et al., 2012). It is built mainly of a Precambrian metamorphic basement upon which Cambrian through Middle Ordovician carbonate rocks were deposited. The Lower Paleozoic is, due to the Caledonian Orogeny, directly overlain by alternatingly marine and continental Late Carboniferous to Middle Triassic sediments. After the Late Triassic, a period of exclusively continental deposition started, interrupted by several unconformities due to the Indosinian and Yanshan orogenies. The Ordos Basin owes its final shape to the Late Cenozoic Himalayan Orogeny (Johnson et al., 1989).

The present study was carried out in the Jinjitan Coal Mine (109°49′15.30″ E, 38°30′25.19″ N), which is located in the northeastern margin of the Ordos Basin (Fig. 1B). The Yan' an Formation represents the maximum lacustrine expansion across the Ordos Basin concomitant with tectonic uplift along the western flanks of the basin (Li et al., 1995b). The predominantly coarse-grained fluvial to floodplain deposits of the Middle Jurassic Zhiluo Formation fill the paleovalleys that formed in the underlying Yan an Formation with only minor coal relative to the latter (Li et al., 1995b; Ao et al., 2012). The mega-sequence ends with the purplish-red and variegated sediments (sandstone, mudstone, and marl) of the Anding Formation, which were deposited in a lacustrine setting under semi-arid climate conditions (Zhang et al., 2021). A variety of plant, sporopollen, and freshwater bivalve fossils suggest Early to Middle Jurassic ages for the Fuxian, Yan' an, and Zhiluo Formations (Li et al., 1995a; Wang, 1996; Zhang et al., 1998).

The Yan'an Formation contains five coal seams in the Jinjitan Coal Mine, among which Coal Seam 2 (CB2) is the principal mineable coal seam. This seam is about 8 m thick, and is divided by a thin silty-mudstone layer (~8 cm thick) into a lower and an upper unit (Fig. 2).

3. Material and methods

A total of 24 unweathered samples were collected from CB2, of which 20 coal samples and four samples of silty mudstone samples. The later were from above, in between, and below CB2. The coal samples were collected at intervals of 40 cm and named CB-1 to CB-20 from top to bottom on working face. The silty-mudstone samples were labeled as MS-1 to MS-4 from top to bottom (Fig. 2).

A preliminary analysis of the coal samples was carried out using the 2011 ASTM Standards D3173-11, D3175-11, and D3174-11. The various forms of sulfur and the total sulfur content were determined (Table S1) following the 2002 ASTM Standards D2492-02 and D3177-02, respectively. The mean random reflectance of vitrinite was determined at the Shandong Provincial Key Laboratory of Depositional Mineralization & Sedimentary Minerals using a Zeiss Axio Scope A1 reflected-light microscope equipped with an MSP UV–VIS2000 spectrophotometer.

The concentrations of major-element oxides (SiO_2, TiO_2, Al_2O_3, Fe_2O_3, MnO, MgO, CaO, Na_2O, K_2O, and P_2O_5) in the samples were measured (on ash basis; 960 ℃ ashing temperature) by elemental analysis using a wavelength dispersive X-ray fluorescence spectrometer (XRF-1800). The concentrations of the trace elements in the samples were determined using a high-resolution inductively coupled plasma mass spectrometer (HR-ICP-MS, Element XR) following Dai et al. (2011). The samples were crushed and ground to<200 mesh, and then subjected

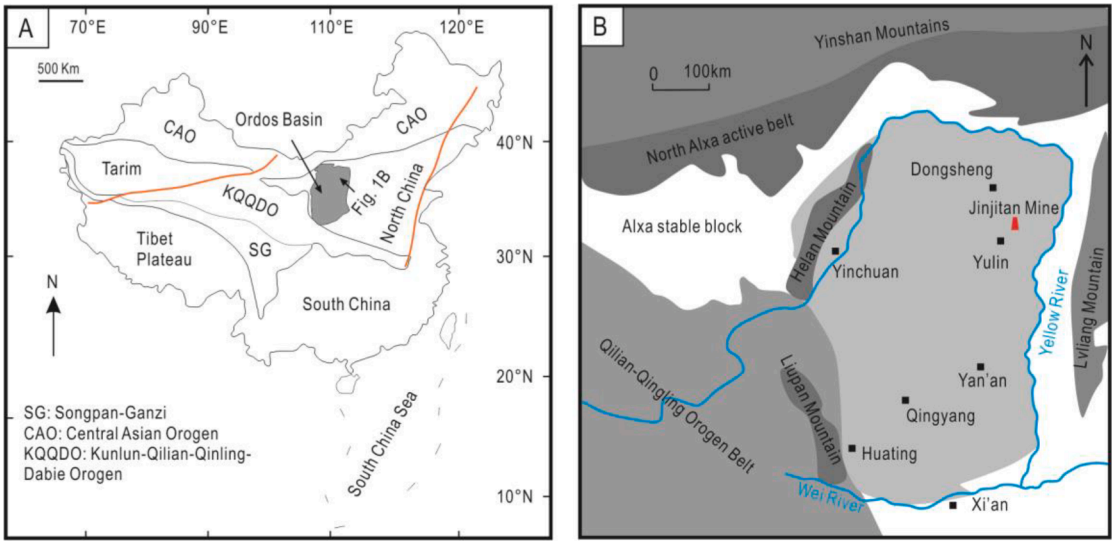

Fig. 1. Location maps. A: Schematic tectonic map of China with location of the Ordos Basin (modified from Darby and Ritts, 2002). B: The Ordos Basin (modified from Liu et al., 2021) with the position of the Jinjitan Coal Mine.

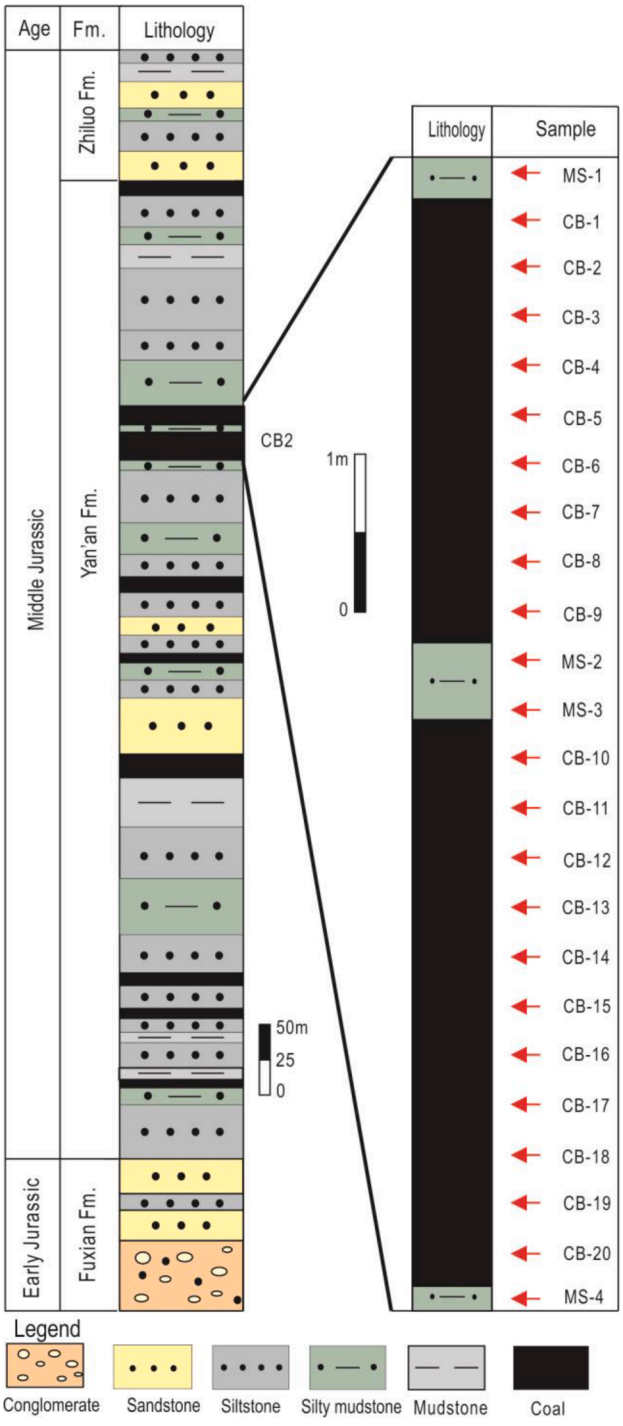

Fig. 2. Simplified sedimentary succession in the Jinjitan Coal Mine showing the position of Coal Seam 2 (CB2) of the Yan'an Formation and stratigraphic levels from which samples were collected from CB2 and its underlying, intercalated and overlying silty mudstones.

for 48 h to digestion in an oven at 190 °C, using mixed acid reagents consisting of 1.5 ml HNO_3 and 1.5 ml HF. The solution was at ~ 140 ℃ to dryness followed by adding 1 ml HNO_3 and evaporating to the second round of dryness, and then redissolved by ~ 3 ml of 30 % HNO_3 and resealed and heated in the bomb at ~ 190 ℃ for 12–24 h. The final solution was diluted to about 100 g using a mixture of 2 % HNO_3 for ICP-MS analysis. The elemental analyses of the samples were completed in the Analytical Laboratory of the Beijing Research Institute of Uranium Geology.

4. Results

The various analyses were aimed at obtaining information that could help interpret the depositional environment(s) and related factors under which the coals were formed. These analyses included (1) the coal chemistry and the vitrinite reflectance, (2) the concentration of major elements in the collected samples, and (3) the concentrations in the samples of REE.

4.1. Coal chemistry and vitrinite reflectance

The results of the chemical analyses of the coal samples of CB2 are presented in Table S1. The ash yield (dry basis, A_d) ranges from 2.40 % to 14.02 %, with an average of 8.38 %. The coals samples thus are low-ash coals according to the 2004 Chinese coal-quality classification (GB/T15224.1). The weighted average vitrinite reflectance (0.56 %) and volatile matter (33.28 %, dry and ash-free basis) of the coal samples indicates a high volatile bituminous rank coal according to the 2015 ASTM classification (ASTM D388-15). The total sulfur content in the coal ranges from 0.08 % to 1.94 %, with an average of 0.48 %, indicating low-sulfur coal (<1 for low-sulfur coal and 1–3 % for medium-sulfur coal: Chou, 2012).

4.2. Concentrations of major elements

SiO_2 and Al_2O_3 are the oxides of the most abundant major elements; to a lesser extent, Fe_2O_3 and CaO are present (Table S2). The contents of Na_2O, K_2O, and MgO are higher than those in most Chinese coals reported by Dai et al. (2012b). The other major-element oxides are either lower or close to those in typical Chinese coals. The SiO_2/Al_2O_3 ratio of the coal (1.76 on average) is higher than that of other Chinese coals (1.42) (Dai et al., 2012b) and also than the theoretical ratio for kaolinite (1.18, Mücke et al., 1999; Burger et al., 2002; Ojo et al., 2017), thus indicating free SiO_2 in the coal (Li et al., 2019).

4.3. Concentrations of trace elements

Compared to the average for world hard coals (Ketris and Yudovich, 2009), a few trace elements are enriched in CB2 (Table S3; Fig. 3). The trace elements with a concentration coefficient (CC = ratio of element concentration in CB2 vs world hard coals) of $5 < CC < 10$ only include Ba. Trace elements with a CC of 2–5 include Mn. Most trace elements, including Sc, V, Cr, Co, Ni, Cu, Zn, Ga, Rb, Y, Zr, Nb, Mo, Sn, Cs, Hf, Ta, Pb, Th, U and total REE, are depleted in CB2 ($CC < 0.5$). The concentrations of Be and Sr are close to the average for world hard coals ($0.5 < CC < 2$).

4.4. Concentrations of rare earth elements

Three types of REE distributions can be distinguished, viz. light (L-type), medium (M−type), and heavy (H-type) distributions. The distinction refers to comparison with the Upper Continental Crust (UCC) (Seredin and Dai, 2012). This geochemical classification of the REE is also used in the present study. The light REE (LREE) comprise La, Ce, Pr, Nd, and Sm; the medium type (MREE) comprises Eu, Gd, Tb, Dy, and Y; and the heavy REE (HREE) comprise Ho, Er, Tm, Yb, and Lu (cf. Seredin and Dai, 2012). Accordingly, three enrichment types are identified, L-type ($La_N/Lu_N > 1$), M−type ($La_N/Sm_N < 1$, $Gd_N/Lu_N > 1$), and H-type ($La_N/Lu_N < 1$), in comparison with the UCC (Seredin and Dai, 2012).

The concentrations and distribution of the REE are different for the coal and the silty mudstone. The concentration of REE in CB2 is 15.17 μg/g (Table S4), which is lower than that of the average value for hard coals worldwide (68.41 μg/g; Ketris and Yudovich, 2009). The REE enrichment pattern in CB2 is of the M−type. The silty mudstones have high REE concentrations 154.07 μg/g in the overlying silty mudstones and 136.56 μg/g in the underlying ones, without a significant difference

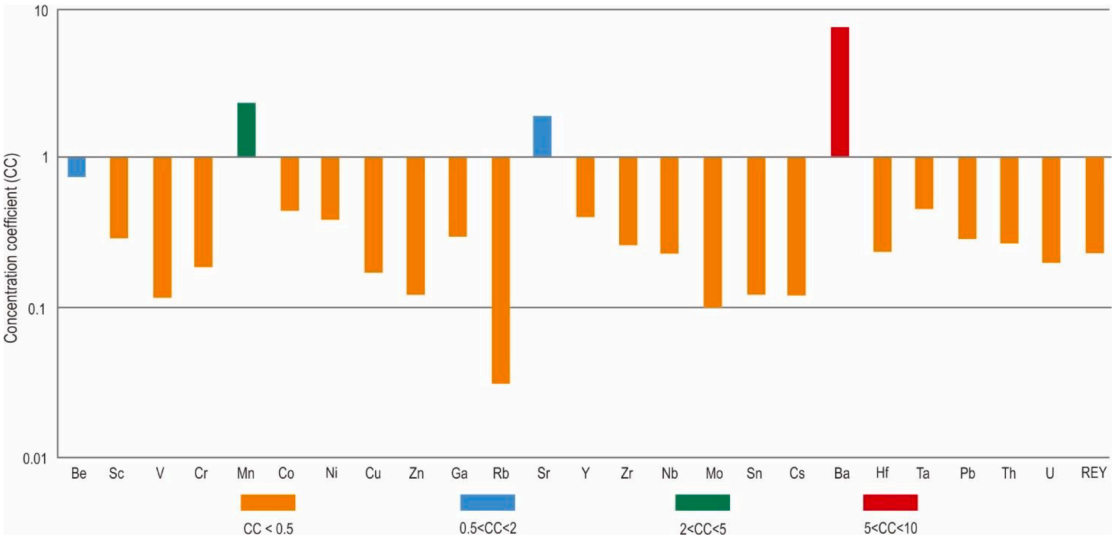

Fig. 3. Concentration coefficients (CC) of trace elements in CB2 of the Yan'an Formation, normalized for the average trace-element concentrations in the world's hard coals (Ketris and Yudovich, 2009).

in REE distribution.

5. Interpretation and discussion

We present here our interpretations of the results in the same order as in Section 4. Because the same geochemical data are frequently interpreted differently in different studies, we discuss our interpretations also in this section, in order to facilitate understanding.

5.1. Major-element geochemistry

Major elements are significant components of the inorganic minerals in the coals. Typically, the elements Si, Al, and Ti are related to detrital minerals such as quartz and clays minerals (Spears and Zheng, 1999; Vassilev and Vassileva, 2007; Fu et al., 2010). The good correlations between the major elements are presented in Fig. 4 and Table S5, indicating that Si, Al, and Ti mainly are present in the mixture of the various clay minerals.

The Na_2O content in the coal samples shows a positive correlation with K_2O ($R^2 = 0.913$), suggesting that they come from the same source (cf. Querol et al., 1997). Na_2O is correlated with SiO_2 and Al_2O_3 (R^2 of 0.5 and 0.53, respectively; Table S5), indicating that the Na is present mainly in clay minerals, rather than in pore water; clay minerals are commonly considered an important Na source in sedimentary rocks (Bai et al., 2015).

CaO is probably present in the inorganic sediment. Moreover, Ca may be present only as CaO in mudstone and coal (Mukhopadhyay et al., 1998). Ning et al. (2022) found that there are many fissure fillings and other calcite crystals in the coals from the northern margin of the Ordos Basin. Therefore, the CaO values likely reflect the presence of calcite, as does MgO, which is highly correlated with CaO ($R^2 = 0.45$). Fe_2O_3 correlates negatively with the total concentrations of Na_2O, K_2O, and TiO_2, but shows a slightly positive correlation with the total sulfur content ($R^2 = 0.39$) (Table S5). The correlation between Fe_2O_3 and Std in this study is up to 0.39. At the location, pyrite was discovered. These suggest that sulfur has promoted the formation of iron sulfide, and that the sulfur content mainly controls the Fe content.

5.2. Trace-element mode of occurrence

The trace elements in coals are commonly believed to be derived from aquatic settings (e.g., a river or delta plain), which promoted material exchange between rock and coal (Shao et al., 2003; Zhang et al., 2004).

Trace elements in coals can mode part of minerals, be bound by organic matter, and be soluted in pore water. Minerals are the primary carrier of trace elements in coals (Gluskoter, 1977; Xu et al., 2004; Raðenoviæ, 2006; Dai et al., 2014; Senior et al., 2020). Correlation analysis is an indirect statistical method to study in which elements occur in coal. After a correlation coefficient has been obtained, the degree of closeness between the two can be determined to measure the genetic relationship between the various trace elements in coals (Mukherjee et al., 1988; Sun et al., 2016; Lin et al., 2017).

According to the correlation coefficient between trace elements and the ash yield (A_d), the trace elements in the coal samples under study here can be divided into two groups (Table S6). Group 1 comprises Sc, Mn, Co, Ni, Zn, Sr, Y, Zr, Nb, Hf, Ta, Pb, Th, and U; they show a low correlation with A_d, suggesting that these elements have a weak inorganic affinity but are related to clay minerals. Group 2 comprises B, V, Cr, Cu, Ga, Rb, Mo, Sn, Cs, and Ba; they have a negative correlation with A_d, indicating that the form in which they occur in coal is poorly correlated with inorganic material, and thus these elements may have a strong organic affinity.

5.3. Distribution and origin of the REE

The REE distribution patterns may help elucidate the genesis and development of sedimentary rocks. Dai et al. (2016) recommended (cf. Taylor and McLennan, 1981) the average composition of the upper continental crust (UCC) as the normalization standard. This is important for coal analysis because material from the UCC is introduced in peat during its formation. The REE distribution patterns in the coal samples are shown in Fig. 5A. The mean UCC values are taken in the present study as the normalization standard reference.

The REE distribution curve (Fig. 5A) is relatively flat, indicating that the internal REE fractionation degree is low. Coal with weak or no differentiation is considered to have a normal enrichment, which is more common in coals with a low REE content than in coals with a high REE content (Dai et al., 2015).

Anomalies in the concentration of several rare earth elements provide specific information about the source and deposition of coals. Particularly noteworthy among them are yttrium, europium, and cerium.

5.3.1. Cerium anomalies in the coal

Several factors, among which the rock geochemistry of the source

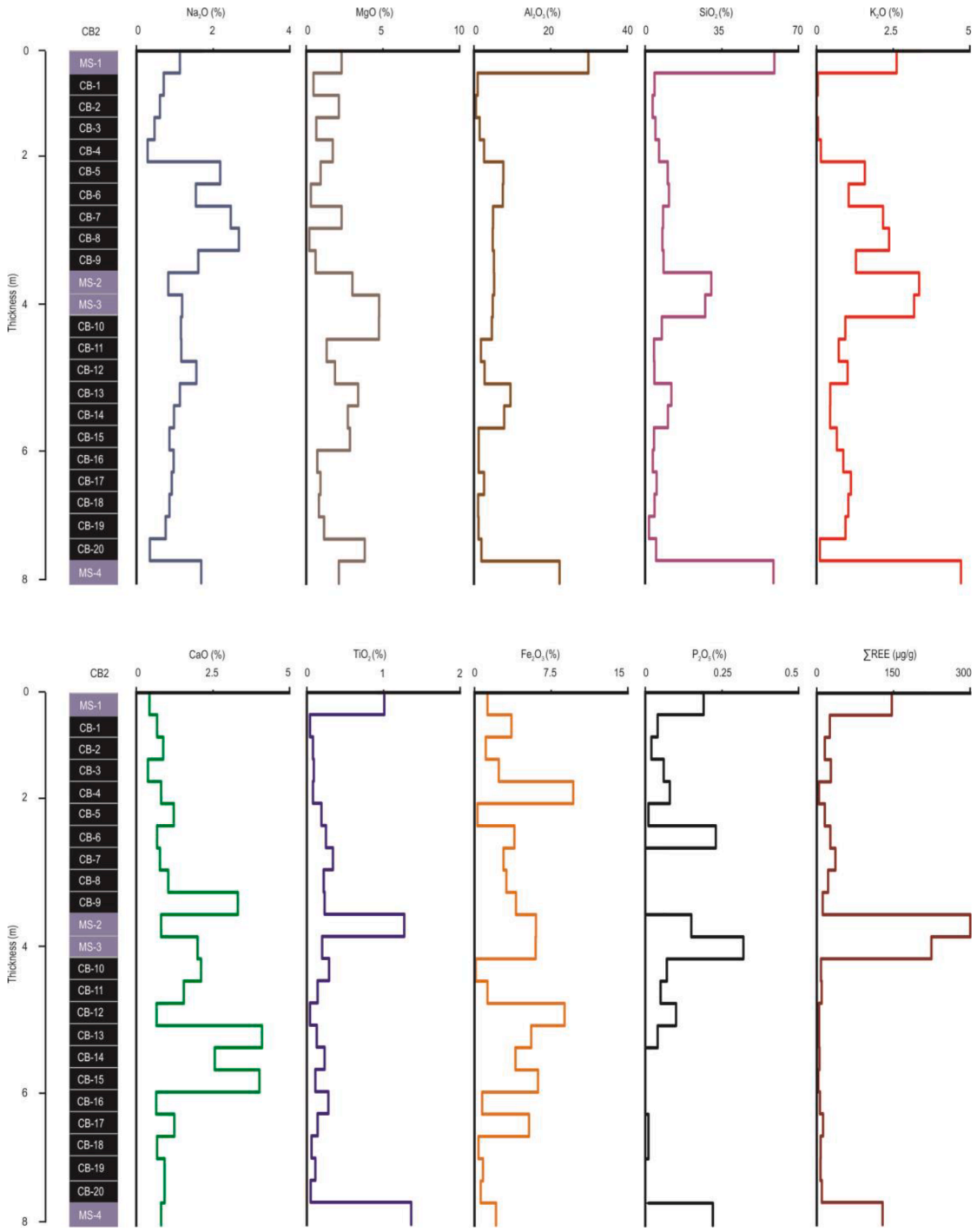

Fig. 4. Vertical variations in CB2 of the major elements and REE.

area, groundwater or hydrothermal leaching, and diagenetic mineralization, may control the Ce characteristics in coal (Leybourne et al., 2000; Zhang et al., 2012; Dai et al., 2016).

The coal samples under study here show slightly negative or no anomalies at all. Coals formed in a marine-influenced environment tend to show negative Ce anomalies (Dai et al., 2016). However, seawater or mineralization cannot have influenced the Ce anomalies of our samples (cf. Kuhn et al., 1998; Dai et al., 2016). Therefore, the geochemical composition of the source area of the clastics within the coals must be an important factor in controlling the Ce anomalies in the studied coal.

5.3.2. Europium anomalies in the coal

Several factors can induce Eu anomalies. Strong positive Eu anomalies can, however, also be artificial: they can be caused by high concentrations of Ba caused by interference from BaO and/or BaOH during ICP-MS analysis (Hower et al., 1999; Zhao et al. 2012; Dai et al., 2015, 2016). Positive Eu anomalies should consequently be considered with great caution in Ba-rich coals (Dai et al., 2016). In our study, the Eu concentration in some samples (MS-4, CB-8, CB-11–18 and CB-20) shows such a strong positive anomaly (Fig. 5A), but the presence of barite may explain this anomaly (Fig. 6A).

The positive correlation between the Ba and Eu concentrations in the coals (Fig. 6B) indicates that Ba has interfered with Eu. The Ba/Eu ratios

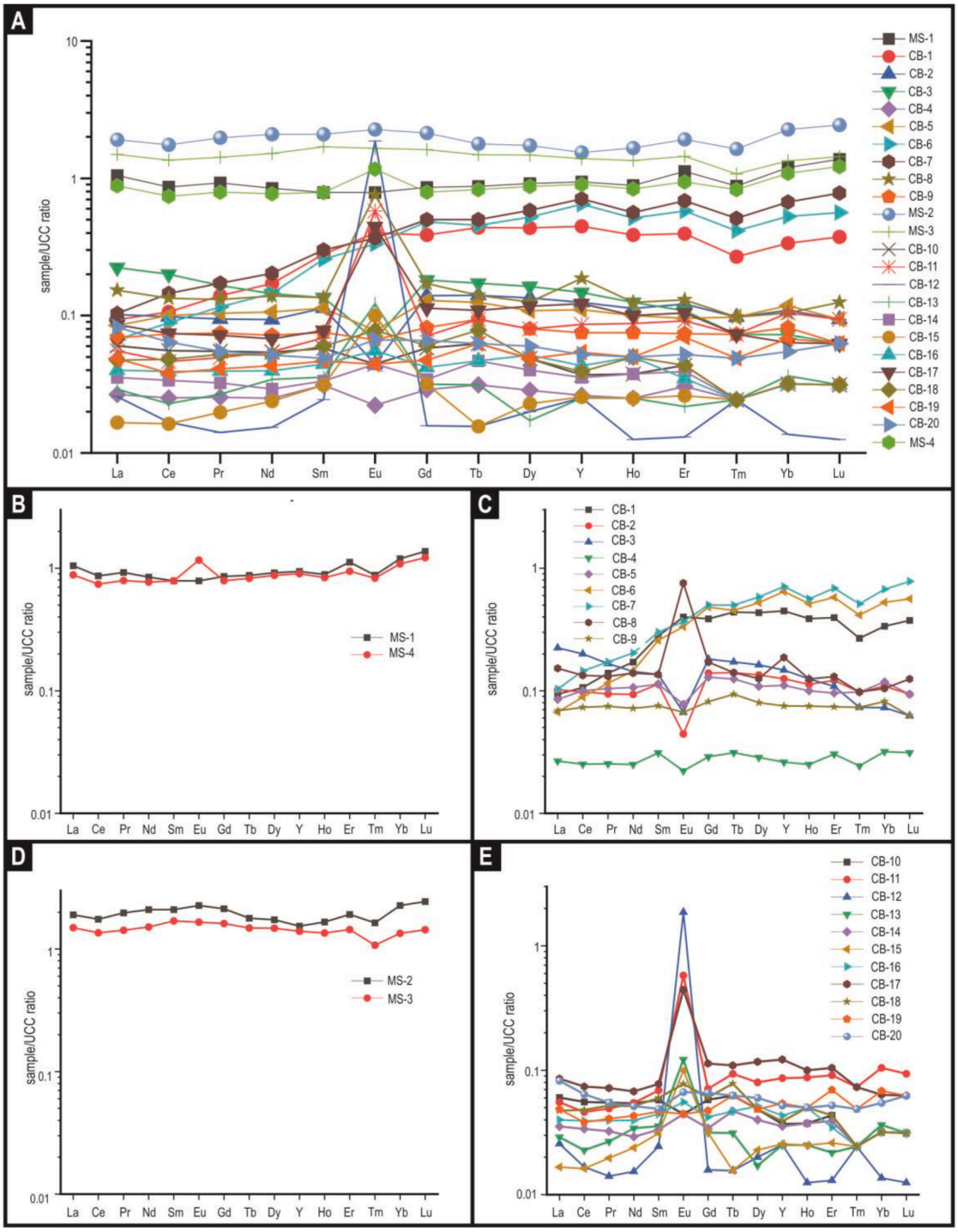

Fig. 5. A: Distribution of the rare earth elements in CB2. B: REE concentrations in the silty mudstones under- and overlying the coals of CB2. C: REE concentrations in the silty-mudstone intercalation of CB2. D: REE concentrations in the upper part of CB2. E: concentrations in the lower part of CB2. REE concentration in CB2 normalized for the Upper Continental Crust (UCC) (Taylor and Mclennan, 1985).

in the coal samples vary from 13.98 to 6728.49, averaging 2111.37. Because this ratio is significantly higher than the interference threshold of 1000 proposed by Dai et al. (2016) and Yan et al. (2019), the strongly positive Eu anomaly is probably an artefact, not representing the actual value (ef. MS-1, CB-1, CB-8, CB-9, CB-11 to CB-15, CB-17, CB-18, CB-20, MS-4).

Some anomalies in other samples (CB-2 to CB-7, MS-2, MS-3, CB-10, CB-16, CB-19, and CB-19) below the interference threshold of 1000 Ba/Eu ratio may have been caused by weathering of the sediment in the source area or during transport from the source area to the peat swamp; moreover, these anomalies may have been inherited from rocks within the source area (e.g., Eskenazy, 1987; Qi et al., 2007; Yossifova et al., 2011; Dai et al., 2015), or positive Eu animalies may have been caused by exposure to high-temperature hydrothermal fluids (e.g., Michard and Albarède, 1986; Bau, 1991; Bau et al., 2014; Dai et al., 2016). High apatite contents of the coals may also result in positive Eu anomalies (mostly $Eu_N/Eu_N^*>1$) (Dai et al., 2016).

On the other hand, distinctly negative Eu anomalies (Fig. 5A, C, E) may have been caused by interference with tonsteins derived from air-borne pyroclastics from alkali rhyolites (Zhang et al, 2021, 2022),

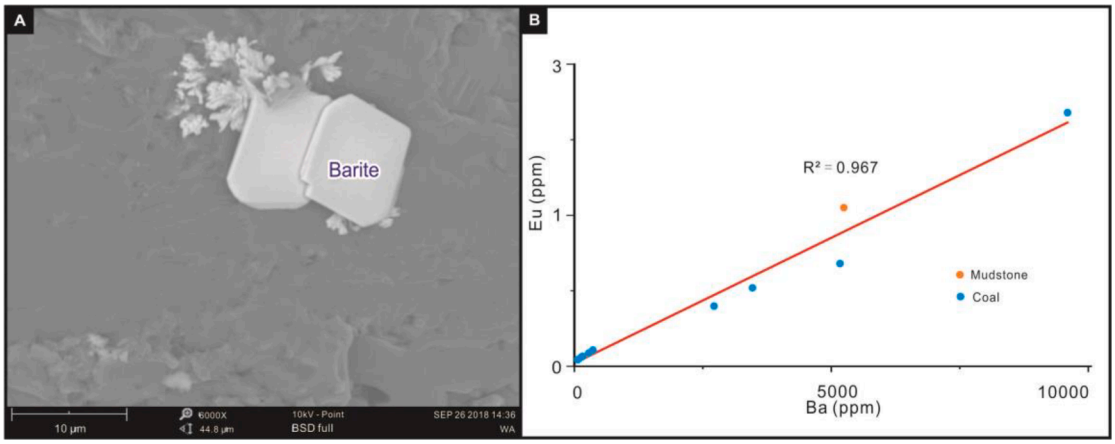

Fig. 6. A: SEM backscattered electron image of barite showing the well-developed crystal morphology. B: Relationship between Eu and Ba in the samples.

volcanogenic hydrothermal solutions, or felsic or felsic/intermediate continental material (Dai et al., 2016). Additionally, the source area has various rock types (such as igneous and pyroclastic rocks with carbonate layers) that have the possibility of causing Eu negative anomalies (Min et al., 2005; Dai et al., 2016).

5.3.3. *Yttrium anomalies in the coal*

Yttrium shows slightly positive or no anomalies at all in the coal

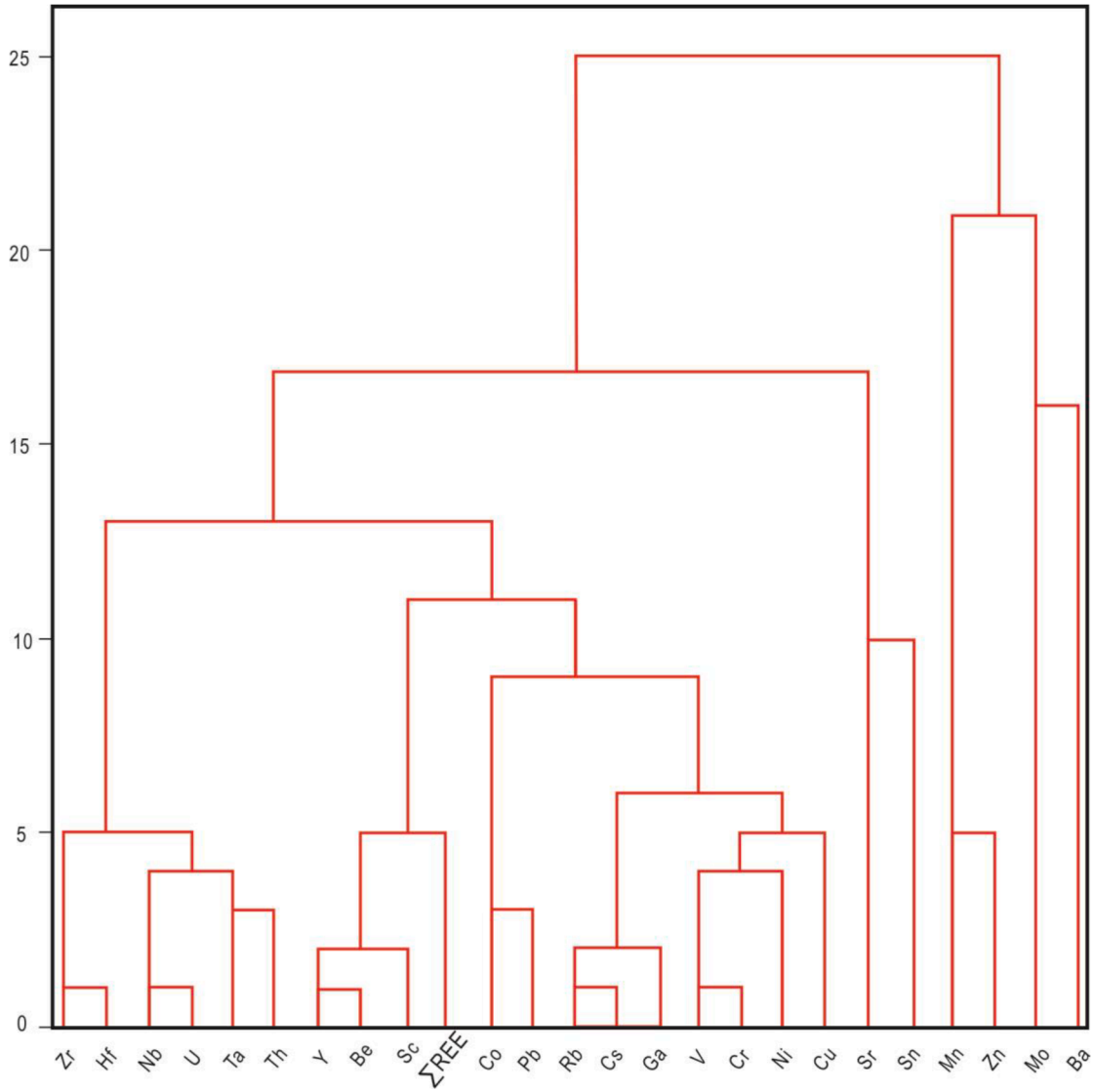

Fig. 7. Cluster analysis of the trace elements, including REE, in CB2.

samples from CB2. Two factors might be responsible: (1) the input of eroded basaltic or felsic/intermediate material; and (2) supply of Y-bearing phosphates from the source area (Dai et al., 2016).

5.3.4. Sources of the REE

REE have unique geochemical characteristics, but similar chemical properties, and low solubility (Middelburg et al., 1988; Šmuc et al., 2012; Khan et al., 2017). Moreover, they remain stable during weathering, erosion, transport, deposition, and early diagenesis. Therefore, the REE are very effective in tracing the source rocks of clastic sediments and thus also in revealing the source area (Munksgaard et al., 2003; Ferrat et al., 2011; Wu et al., 2019). The Ce anomaly (Ce_N/Ce_N^*) can often be used as a signature of seawater (Murray et al., 1990). In addition, LREE and HREE are enriched in seawater, but the total REE concentration is relatively low (Birk and White, 1991). The coal and silty-mudstone samples under study show no distinct Ce anomaly or LREE nor HREE enrichment. This implies that seawater can be excluded as the source of the REE in the succession under study here.

In order to verify this finding, a cluster analysis of REE with continental and non-continental elements has been prepared, with corresponding high field strength elements and large-ion lithophile elements, respectively (Fig. 7). The high field strength elements (Sc, Ti, Y, Zr, Nb, Hf, and Ta) and part of the large-ion lithophile elements (e.g., Rb, Ga, Cs) are inactive during weathering, so that they become adsorbed or combined into particles, then transported and deposited with them (Taylor and McLennan, 1981; Singh and Rajamani, 2001). The REE of the coals show a closer affinity with the high field strength elements (e.g., Sc, Y, Nb, Ta, Th) and a significant affinity with large-ion lithophile elements (e.g., Rb, Ga, Cs, Pb) as well as with elements from eroded rocks (e.g., Li, Co, Zn, Tl, Cr). In contrast, the correlation between REE and elements with another origin (e.g., Mo, Cd, Sr, Sb, Ni) is less strong. This implies that the REE in the coals are derived from eroded rocks in the hinterland.

5.4. Distribution and occurrence of the REE

The REE in the coal samples range from 3.47 to 44.4 μg/g, with an average of 15.17 μg/g, which is far lower than the world average (68.41 μg/g: Ketris and Yudovich, 2009). The vertical distribution of the REE is shown in Fig. 4. Overall, the REE content of the upper part of CB2 is higher than that of the lower part. In non-coal samples, the middle has a larger concentration of REEs than the roof and floor. The REE occur mainly in fine-grained minerals and organic matter. Therefore, the REE increase in the upper part of CB2 must be ascribed to such components. The increase in REE from CB-9 to CB-4 corresponds to the increasing concentrations of Na_2O, Al_2O_3, SiO_2, K_2O, and TiO_2, from eroded clastic rocks. However, the lower part of CB2 (with samples CB-20 to CB-10) shows fluctuations without distinct regularities of Na_2O, Al_2O_3, SiO_2, K_2O, and TiO_2, suggesting that the type of sediment in the various layers controls this uneven distribution.

Comparison of the REE and the major elements shows that the REE in the coal samples are positively correlated with Na_2O, Al_2O_3, SiO_2, K_2O, and TiO_2 (Table S5). HREE is more closely related to Na_2O, Al_2O_3, SiO_2, K_2O, and TiO_2 than LREE. Na_2O, Al_2O_3, SiO_2, K_2O, and TiO_2 were mainly supplied from eroded source rocks during peat accumulation. REEs in coal can be found in diagenetic or late diagenetic stage authigenic minerals like phosphate or sulfate minerals (Seredin and Dai, 2012). However, CB2 of the Yan' an Formation is mainly in the early diagenesis stage (see Section 5.4). As a result, the enrichment of LREE and reduction of HREE in coals must be attributed mostly to clay minerals.

5.5. Geological implications

Seredin and Dai (2012) proposed four genetic types of REE accumulation in coal: (1) a continental type, with REE input by surface water, influenced by the composition of the rocks in the source area, during peat formation; (2) a tuffaceous type, connected with settling and leaching of acid and alkaline volcanic ash, influenced by the composition of the volcanic type, during peat formation; (3) a type driven by infiltration or meteoric groundwater; and (4) a hydrothermal type, related to ascending flows of thermal mineral water and other deep fluids. Just like the major oxides, minor and other trace elements, the REE occurrences must therefore be considered to reflect the provenance area, the depositional environment, and the diagenetic history.

5.5.1. Provenance

Rare earth elements have a strong inheritance and can more accurately reflect the provenance composition (Bhatia and Crook, 1986). Rare earth elements in coal have special geochemical characteristics, such as a high degree of homogenization and stable chemical properties, and they are not easily affected by metamorphism, diagenesis, and alteration, which can more accurately reflect the provenance composition and play an important role in determining the tectonic environment of the source rocks (Taylor and McLennan, 1985; McLennan, 2018). The elemental enrichment of coal during peat accumulation and coalification is controlled by multiple factors (Dai et al., 2012a). According to Wang (1996), the composition of the source tocks in the source area of the clastic components is the main factor that controlled the enrichment and distribution of trace elements in the coal of the Yan'an Formation.

The Al_2O_3/TiO_2 ratio can be used to trace the source area (He et al., 2010). This has been shown, for instance, for the source of volcanic-ash particles in coal and coal-bearing successions (Dai et al., 2016). The Al_2O_3/TiO_2 ratios in sedimentary rock are typically 3–8, 8–21, and 21–70 for source areas consisting of mafic, intermediate, and felsic igneous rocks, respectively (Dai et al., 2016). The Yan'an coal samples have Al_2O_3/TiO_2 ratios ranging from 4.32 to 73, with three samples range 3–8, nine samples range 8–21 and others range 21–70, indicating that the source areas were mostly felsic igneous rocks and intermediate rocks (Fig. 8A), which is also supported by the TiO_2/Zr ratios (Fig. 8B). The lower part is primarily felsic and intermediate rocks. In the upper part, there are more mafic rocks mixed in. Overall, the clastic in the coal of the Yan'an Formation appears to derive mostly from felsic rocks and intermediate rocks with minor amounts of mafic rocks.

5.5.2. Tectonic setting

The Zr/Sc and Th/Sc ratios are considered to reflect the composition, sorting, and heavy-mineral content in sediments (McLennan et al., 1993; Das et al., 2006; Nagarajan et al., 2015) (Fig. 9A). The Zr/Sc vs Th/Sc ratios in this figure show that the sediments of the Yan'an Formation are mainly derived from felsic rocks, and that most sediments did not experience significant recycling. Therefore, the geochemical data of these sediments can be used to analyze the tectonic setting of the source area.

Stable elements can effectively help to trace the provenance area on the basis of the REE concentrations and ratios (McLennan et al., 1993; Kasanzu et al., 2008). The relationships of La/Th–Hf (Floyd and Leveridge, 1987), La/Sc–Co/Th (Wronkiewicz and Condie, 1987), and La/Yb-REE (Allegre and Minster, 1978) are used to analyze the source rocks (Bai et al., 2015). Comprehensive analysis shows that the Yan'an Formation is mainly composed of the felsic volcanic rocks and granite, mixed with small amounts of intermediate and mafic igneous rocks and sedimentary rocks (Fig. 9B-D). The maximally slightly negative Ce anomalies support this conclusion (Fig. 5A-B) because weakly negative Ce anomalies characterize source areas dominated by felsic or felsic/intermediate rocks and weak or no Y anomalies (Dai et al., 2016).

Some trace elements are inactive during transport and deposition, reflecting the tectonic setting better (Bhatia, 1985; Lv et al., 2019; Mirza et al., 2021). Diagrams of La-Th-Sc, Th-Sc-Zr/10, and Th-Co-Zr/10 (Bhatia and Crook, 1986) show that most samples are located on a continental island arc, whereas few samples present active continental margin setting (Fig. 9E–G).

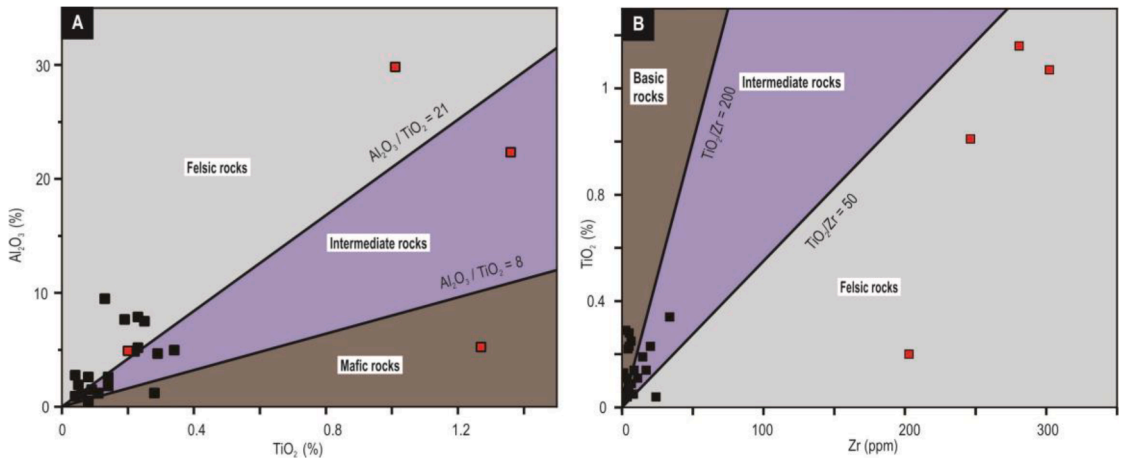

Fig. 8. Probable type of source rocks of the clastic material in CB2 as indicated by elemental ratios. A: Al_2O_3 *versus* TiO_2. B: TiO_2 *versus* Zr. Black and red solid squares represent coal and silty-mudstone samples, respectively. (For interpretation of the references to colour in this figure legend, the reader is referred to the web version of this article.)

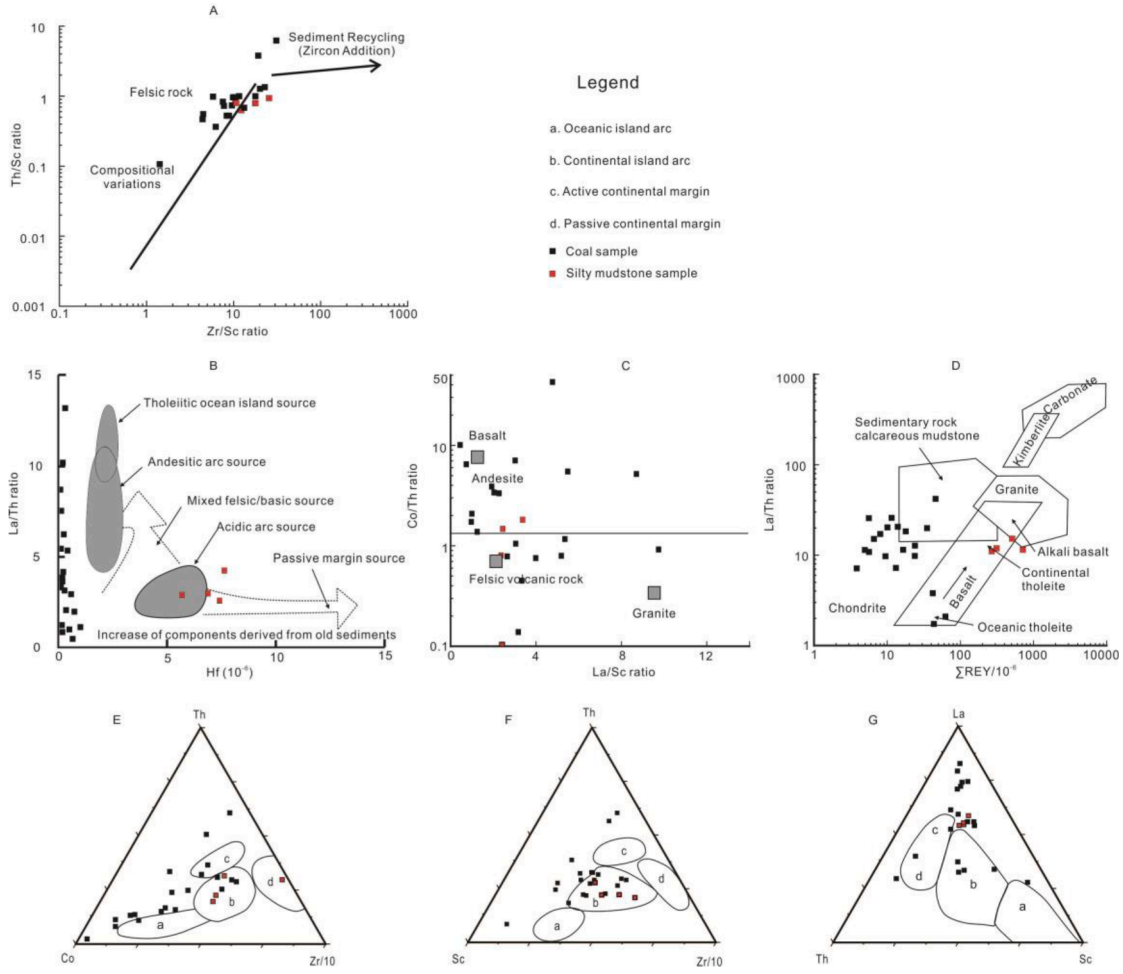

Fig. 9. Possible source rocks and tectonic setting of the source area as indicated by geochemical parameters. Base map source for Figure A: McLennan et al. (1993); for Figure B: Floyd and Leveridge (1987); for Figure C: Wronkiewicz and Condie (1987); for Figure D: Allegre and Minster (1978); for Figures E, F, and G: Bhatia and Crook (1986).

5.5.3. *Influence of provenance and tectonic setting on coal formation*

Provenance can be reflected by the REE in coals (Dai et al., 2012b; Seredin and Dai, 2012). The source area of clastic deposits of the Yan'an Formation in the northern and eastern parts of the Ordos Basin has thus been investigated, suggesting that the source rocks of the clastic deposits of the Yan'an Formation there were Archean and Early Proterozoic granites and granite-gneisses in the Yinshan Mountains, Lvliang Mountains, and in an area around Alxa in the north of the Ordos Basin (Huang

et al., 2009; Lei et al., 2017; Zhang et al., 2022). This finding seems also applicable to the study area, as indicated by a comparison of the REE in the silty mudstones with the study by Huang et al. (2009) (Fig. 10A).

There is still an unsolved problem, however: it is not yet well established whether the source areas remained the same during the entire time-span of coal formation. In order to solve this problem, we compared the REE occurrences in the coals with those of the silty mudstones. This analysis revealed differences in type and concentrations of the various REE specimens. We also found that the REE contents in our coal samples differ from those in the coals from the northern margin of the Ordos Basin that were investigated by Wang et al. (2022).

The REE in the northern Ordos Basin show enrichment of the LREE (La, Ce, Pr, Nd, and Sm), whereas our coal samples show enrichment of the MREE (Eu, Gd, Tb, Dy, and Y, see Section 4.4, Table S4). This suggests a source area that was not same as that the Yan'an Fm. in the northern Ordos Basin. This implies that different provenances areas should be considered when studying the depositional environments of coal-bearing successions that extend over a wide area.

The diagram of trace and rare earth elements (Fig. 10B) shows that the tectonic setting was mainly an active continental margin associated with continental island arcs. This indicates that the Yan'an Formation has probably several source areas. It has been hypothesized that the increasing weathering induced by climate change resulted in more source rocks, which influenced the coal quality (Zhang et al., 2021). Climate change may thus be one of the main geological factors that controlled the weathering of the source area.

5.6. Diagenesis

Shields and Stille (2001) suggested that diagenesis can change the Ce anomaly and lead to a stronger positive correlation between Ce/Ce^*_N and Eu/Eu^*_N, as well as between Ce/Ce^*_N and REE, and to a negative correlation between Ce/Ce^*_N and Dy_N/Sm_N. The coals thus have a relatively poor correlation between Ce/Ce and Eu/Eu^*_N ($R^2 = 0.14$) and between Ce/Ce^*_N and the REE ($R^2 = 0.05$), which shows weak diagenesis (Table S4). The V/Cr ratio lower than 2.0 reflects, however, that the sediments have experienced a certain degree of diagenesis (Trueman and Tuross, 2002). Combination of these findings indicates that the coals of CB2 have undergone early diagenesis.

6. Conclusions

The main findings of the present study can be summarized in the following five conclusions concerning CB2 of the Yan'an Formation in the study area.

Major-elements are primarily from the mixuture of various clay minerals. Ca occurs mainly in calcite. The iron distribution is controlled mainly by sulfur due to the better correlation between Fe_2O_3 and S_{td}. The trace elements are, except for Mn, Ba, B, and Sr, all below the average world values for coal.

The REE content of the upper part of CB2 is higher than that of the lower part, which may be due to increased input of eroded clastic material. REE distribution pattern is relatively flat. LREE is slightly enriched, which is a normal situation. Eu shows anomalies; the negative anomalies can be attributed to the input of felsic or felsic/intermediate eroded material, whereas positive anomalies may be due to the presence of barite or apatite. The Y no anomalies may be induced by input of erosion products with TiO_2 minerals, phosphates, and zircon. The cluster analysis between REE and trace elements shows that the input of eroded material must be the source of the REE in the coals.

With only a minor number of mafic rocks and sedimentary rocks, the clastic particles in CB2 are primarily produced from felsic volcanic rocks and intermediate rocks. The source rocks are primarily situated in the tectonic setting of a continental inland arc.

The provenance of the studied succession of the Yan'an Formation was predominantly the northern margin of the Ordos Basin, but there were several other source areas. Climate change seems to have been the main geological factor controlling the peat accumulation.

Declaration of Competing Interest

The authors declare that they have no known competing financial

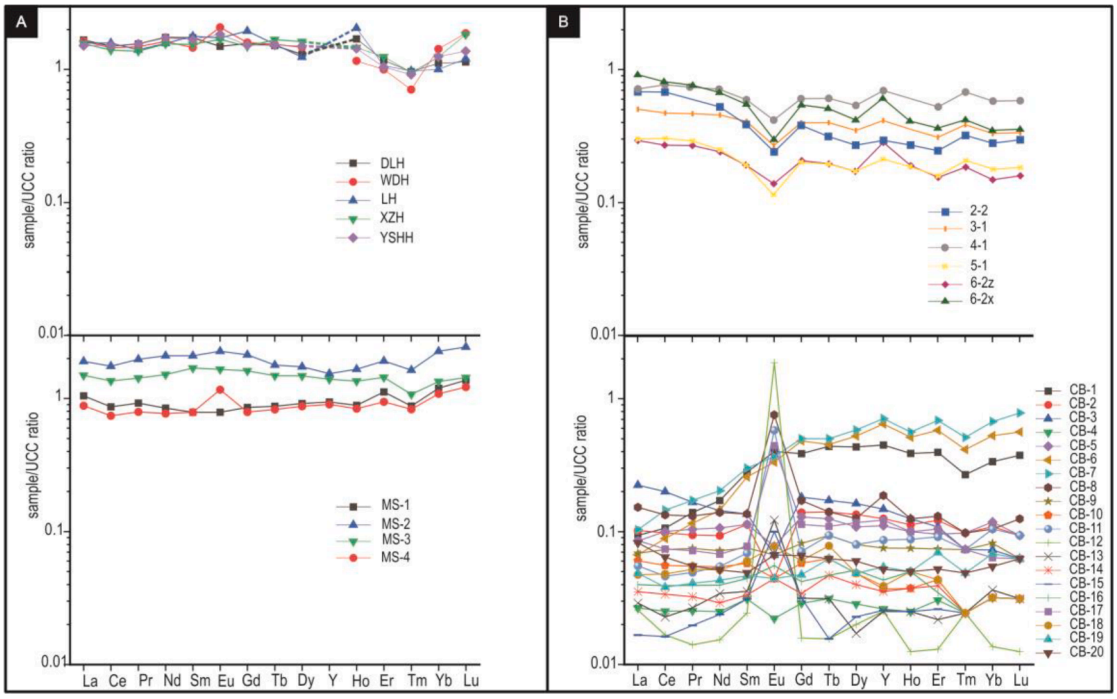

Fig. 10. Possible source areas as based on the comparison of trace- element concentrations. A: Comparison between silty mudstones from (top) the eastern margin of the Ordos Basin (Huang et al., 2009) and (bottom) silty-mudstone samples from the present study. B: Comparison between coals from (top) the northern margin of the Ordos Basin (Wang et al., 2022) and (bottom) coal samples from the present study.

interests or personal relationships that could have appeared to influence the work reported in this paper.

Data availability

Data will be made available on request.

Acknowledgments

We would like to thank Associate Editor Hao Zou, and three anonymous reviewers for their constructive comments. This study was financially supported by the National Key R&D Plan of China (Grant No. 2017YFC0601405), the National Natural Science Foundation of China (Grants No. 41772096 and 42102127), the SDUST Research Fund (Grant No. 2018TDJH101) and the Shandong Provincial Natural Science Foundation (Grant No. ZR2021QD087).

Appendix A. Supplementary data

Supplementary data to this article can be found online at https://doi.org/10.1016/j.oregeorev.2022.105218.

References

Allegre, C., Minster, J., 1978. Quantitative models of trace element behavior in magmatic processes. Earth Planet. Sci. Lett. 38, 1–25.
Ao, W., Huang, W., Weng, C., Xiao, X., Liu, D., Tang, X., Chen, P., Zhao, Z., Wan, H., Finkelman, R.B., 2012. Coal petrology and genesis of Jurassic coal in the Ordos Basin, China. Geoscience 3, 85–95.
Arbuzov, S.I., Chekryzhov, I.Y., Finkelman, R.B., Sun, Y.Z., Zhao, C.L., Il'enok, S.S., Blokhin, M.G., Zarubina, N.V., 2019. Comments on the geochemistry of rare-earth elements (La, Ce, Sm, Eu, Tb, Yb, Lu) with examples from coals of north Asia (Siberia, Russian far East, North China, Mongolia, and Kazakhstan). Int. J. Coal Geol. 206, 106–120.
Bai, Y., Liu, Z., Sun, P., Liu, R., Hu, X., Zhao, H., Xu, Y., 2015. Rare earth and major element geochemistry of Eocene fine-grained sediments in oil shale- and coal-bearing layers of the Meihe Basin, Northeast China. J. Asian Earth Sci. 97, 89–101.
Balaram, V., 2019. Rare earth elements: a review of applications, occurrence, exploration, analysis, recycling, and environmental impact. Geoscience 10, 1285–1303.
Bau, M., 1991. Rare-earth element mobility during hydrothermal and metamorphic fluid-rock interaction and the significance of the oxidation state of europium. Chem. Geol. 93, 219–230.
Bau, M., Schmidt, K., Koschinsky, A., Hein, J., Kuhn, T., Usui, A., 2014. Discriminating between different genetic types of marine ferro-manganese crusts and nodules based on rare earth elements and yttrium. Chem. Geol. 381, 1–9.
Bhatia, M.R., 1985. Rare earth element geochemistry of Australian Paleozoic graywackes and mudrocks: provenance and tectonic control. Sediment. Geol. 45, 97–113.
Bhatia, M.R., Crook, K.A., 1986. Trace element characteristics of graywackes and tectonic setting discrimination of sedimentary basins. Contrib. Mineral. Petrol. 92, 181–193.
Bhattacharjee, J., Ghosh, K.H., Bhattacharya, B., 2018. Petrography and geochemistry of sandstone–mudstone from Barakar Formation (early Permian), Raniganj Basin, India: Implications for provenance, weathering and marine depositional conditions during Lower Gondwana sedimentation. Geol. J. 53, 1102–1122.
Birk, D., White, J.C., 1991. Rare earth elements in bituminous coals and underclays of the Sydney Basin, Nova Scotia: Element sites, distribution, mineralogy. Int. J. Coal Geol. 19, 219–251.
Burger, K., Zhou, Y., Ren, Y., 2002. Petrography and geochemistry of tonsteins from the 4th Member of the Upper Triassic Xujiahe Formation in southern Sichuan Province, China. Int. J. Coal Geol. 49, 1–17.
Chou, C.-L., 2012. Sulfur in coals: A review of geochemistry and origins. Int. J. Coal Geol. 100, 1–13.
Dai, S., Wang, X., Zhou, Y., Hower, J.C., Li, D., Chen, W., Zhu, X., Zou, J., 2011. Chemical and mineralogical compositions of silicic, mafic, and alkali tonsteins in the late Permian coals from the Songzao Coalfield, Chongqing, southwest China. Chem. Geol. 282, 29–44.
Dai, S., Ren, D., Chou, C.-L., Finkelman, R.B., Seredin, V.V., Zhou, Y., 2012a. Geochemistry of trace elements in Chinese coals: a review of abundances, genetic types, impacts on human health, and industrial utilization. Int. J. Coal Geol. 94, 3–21.
Dai, S., Wang, X., Seredin, V.V., Hower, J.C., Ward, C.R., O'Keefe, J.M., Huang, W., Li, T., Li, X., Liu, H., 2012b. Petrology, mineralogy, and geochemistry of the Ge-rich coal from the Wulantuga Ge ore deposit, Inner Mongolia, China: New data and genetic implications. Int. J. Coal Geol. 90, 72–99.
Dai, S., Zhang, W., Ward, C.R., Seredin, V.V., Hower, J.C., Li, X., Song, W., Wang, X., Kang, H., Zheng, L., 2013. Mineralogical and geochemical anomalies of late Permian coals from the Fusui Coalfield, Guangxi Province, southern China: influences of terrigenous materials and hydrothermal fluids. Int. J. Coal Geol. 105, 60–84.
Dai, S., Luo, Y., Seredin, V.V., Ward, C.R., Hower, J.C., Zhao, L., Liu, S., Zhao, C., Tian, H., Zou, J., 2014. Revisiting the late Permian coal from the Huayingshan, Sichuan, southwestern China: Enrichment and occurrence modes of minerals and trace elements. Int. J. Coal Geol. 122, 110–128.
Dai, S., Yang, J., Ward, C.R., Hower, J.C., Liu, H., Garrison, T.M., French, D., O'Keefe, J. M., 2015. Geochemical and mineralogical evidence for a coal-hosted uranium deposit in the Yili Basin, Xinjiang, northwestern China. Ore Geol. Rev. 70, 1–30.
Dai, S., Liu, J., Ward, C.R., Hower, J.C., French, D., Jia, S., Hood, M.M., Garrison, T.M., 2016. Mineralogical and geochemical compositions of Late Permian coals and host rocks from the Guxu Coalfield, Sichuan Province, China, with emphasis on enrichment of rare metals. Int. J. Coal Geol. 166, 71–95.
Darby, B.J., Ritts, B.D., 2002. Mesozoic contractional deformation in the middle of the Asian tectonic collage: the intraplate Western Ordos fold–thrust belt. China. Earth Planet. Sci. Lett. 205, 13–24.
Das, B.K., Al-Mikhlafi, A., Kaur, P., 2006. Geochemistry of Mansar Lake sediments, Jammu, India: Implication for source-area weathering, provenance, and tectonic setting. J. Asian Earth Sci. 26, 649–668.
Der Flier-Keller, V., 1993. Earth elements in western Canadian coals. Energy Sources 15, 623–638.
Dushyantha, N., Batapola, N., Ilankoon, I., Rohitha, S., Premasiri, R., Abeysinghe, B., Ratnayake, N., Dissanayake, K., 2020. The story of rare earth elements (REEs): Occurrences, global distribution, genesis, geology, mineralogy and global production. Ore Geol. Rev. 122, 103521.
Eskenazy, G.M., 1987. Rare earth elements and yttrium in lithotypes of Bulgarian coals. Org. Geochem. 11, 83–89.
Ferrat, M., Weiss, D.J., Strekopytov, S., Dong, S., Chen, H., Najorka, J., Sun, Y., Gupta, S., Tada, R., Sinha, R., 2011. Improved provenance tracing of Asian dust sources using rare earth elements and selected trace elements for palaeomonsoon studies on the eastern Tibetan Plateau. Geochim. Cosmochim. Acta 75, 6374–6399.
Floyd, P., Leveridge, B., 1987. Tectonic environment of the Devonian Gramscatho Basin, south Cornwall: framework mode and geochemical evidence from turbiditic sandstones. J. Geol. Soc. London 144, 531–542.
Fu, X., Wang, J., Zeng, Y., Tan, F., Feng, X., 2010. REE geochemistry of marine oil shale from the Changshe Mountain area, northern Tibet. China. Int. J. Coal Geol. 81, 191–199.
Gluskoter, H.J., 1977. Trace elements in coal: occurrence and distribution. Illinois State Geologicl Survey Circular 499 pp.
Guo, P., Liu, C., Wang, J., Deng, Y., Mao, G., Wang, W., 2018. Detrital-zircon geochronology of the Jurassic coal-bearing strata in the western Ordos Basin, North China: Evidences for multi-cycle sedimentation. Geoscience 9, 1725–1743.
He, B., Xu, Y.-G., Zhong, Y.-T., Guan, J.-P., 2010. The Guadalupian-Lopingian boundary mudstones at Chaotian (SW China) are clastic rocks rather than acidic tuffs: implication for a temporal coincidence between the end-Guadalupian mass extinction and the Emeishan volcanism. Lithos 119, 10–19.
Hower, J.C., Ruppert, L.F., Eble, C.F., 1999. Lanthanide, yttrium, and zirconium anomalies in the Fire Clay coal bed, Eastern Kentucky. Int. J. Coal Geol. 39, 141–153.
Hower, J.C., Groppo, J.G., Henke, K.R., Hood, M.M., Eble, C.F., Honaker, R.Q., Zhang, W., Qian, D., 2015. Notes on the potential for the concentration of rare earth elements and yttrium in coal combustion fly ash. Minerals 5, 356–366.
Hower, J.C., Granite, E.J., Mayfield, D.B., Lewis, A.S., Finkelman, R.B., 2016. Notes on contributions to the science of rare earth element enrichment in coal and coal combustion byproducts. Minerals 6, 32.
Huang, G., Zhou, X., Wang, Z., 2009. Provenance analysis of the Yan'an Formation in Mid-Jurassic at the southeast area of Ordos Basin. Bull. Mineral. Petrol. Geochem. 28, 252–258.
Johnson, E.A., Liu, S., Zhang, Y., 1989. Depositional environments and tectonic controls on the coal-bearing Lower to Middle Jurassic Yan'an Formation, southern Ordos Basin, China. Geology 17, 1123–1126.
Kasanzu, C., Maboko, M.A., Manya, S., 2008. Geochemistry of fine-grained clastic sedimentary rocks of the Neoproterozoic Ikorongo Group, NE Tanzania: Implications for provenance and source rock weathering. Precambr. Res. 164, 201–213.
Kato, Y., Fujinaga, K., Nakamura, K., Takaya, Y., Kitamura, K., Ohta, J., Toda, R., Nakashima, T., Iwamori, H., 2011. Deep-sea mud in the Pacific Ocean as a potential resource for rare-earth elements. Nat. Geosci. 4, 535–539.
Ketris, M.á., Yudovich, Y.E., 2009. Estimations of Clarkes for Carbonaceous biolithes: World averages for trace element contents in black shales and coals. Int. J. Coal Geol. 78, 135-148.
Khan, A.M., Bakar, N.K.A., Bakar, A.F.A., Ashraf, M.A., 2017. Chemical speciation and bioavailability of rare earth elements (REEs) in the ecosystem: a review. Environ. Sci. Pollut. Res. 24, 22764–22789.
Kuhn, T., Bau, M., Blum, N., Halbach, P., 1998. Origin of negative Ce anomalies in mixed hydrothermal–hydrogenetic Fe–Mn crusts from the Central Indian Ridge. Earth Planet. Sci. Lett. 163, 207–220.
Lei, K., Liu, C., Zhang, L., Wu, B., Cun, X., Sun, L., 2017. Element geochemical characteristics of the Jurassic mudstones in the northern Ordos Basin: Implications for tracing sediment sources and paleoenvironment restoration. Acta Sediment. Sinica 35, 621–636 (in Chinese with English abstract).
Leybourne, M.I., Goodfellow, W.D., Boyle, D.R., Hall, G.M., 2000. Rapid development of negative Ce anomalies in surface waters and contrasting REE patterns in groundwaters associated with Zn–Pb massive sulphide deposits. Appl. Geochem. 15, 695–723.
Li, S., Yang, S., and Jerzykiewicz, T., 1995b, Upper Triassic-Jurassic foreland sequences of the Ordos Basin in China, in Dorobek, S.L., and Ross, G.M., eds., Stratigraphic Evolution of Foreland Basins: Tulsa, Oklahoma, SEPM (Society for Sedimentary Geology) 233-241pp.Lin, R., Bank, T.L., Roth, E.A., Granite, E.J., Soong, Y., 2017.

Organic and inorganic associations of rare earth elements in central Appalachian coal. Int. J. Coal Geol. 179, 295-301.
Li, B., Zhuang, X., Querol, X., Moreno, N., Yang, L., Shangguan, Y., Li., J., 2019. Mineralogy and geochemistry of late permian coals within the Tongzi coalfield in Guizhou province, Southwest China. Minerals, 10, 44.
Li, S., Lin, C., Xie, X., Yang, S., Jiao, Y., 1995. Approaches of nonmarine sequence stratigraphy—A case study on the Mesozoic Ordos Basin. Earth Sci. Front. 2, 133–136.
Lin, R., Bank, T.L., Roth, E.A., Granite, E.J., Soong, Y., 2017. Organic and inorganic associations of rare earth elements in central Appalachian coal. Int. J. Coal Geol. 179, 295–301.
Liu, K., Wang, R., Shi, W., Zhang, W., Qin, S., Qi, R., Xu, L., 2021. Multiple provenance system of Lower Shihezi Formation in Hangjinqi area, northern Ordos Basin: evidence from mineralogy and detrital zircon U-Pb chronology. Earth Sci. 46, 540–554 (in Chinese with English abstract).
Lv, D., Li, Z., Wang, D., Li, Y., Liu, H., Liu, Y., Wang, P., 2019. Sedimentary model of coal and shale in the Paleogene Lijiaya Formation of the Huangxian Basin: insight from petrological and geochemical characteristics of coal and shale. Energy Fuels 33, 10442–10456.
Lv, D., Song, Y., Shi, L., Wang, Z., Cong, P., Van Loon, A.J., 2020. The complex transgression and regression history of the northern margin of the Palaeogene Tarim Sea (NW China), and implications for potential hydrocarbon occurrences. Mar. Pet. Geol. 112, 104041.
Mclennan, S.M., 2018. Rare earth elements in sedimentary rocks: influence of provenance and sedimentary processes, Geochemistry and mineralogy of rare earth elements. De Gruyter, pp. 169–200.
McLennan, S., Hemming, S., McDaniel, D., Hanson, G., 1993. Geochemical approaches to sedimentation, provenance, and tectonics. In: Johnsson, M.J., Basu, A. (Eds.), Processes Controlling the Composition of Clastic Sediments. Geol. Soc. Am. Spec. Pap. 284, 21-40.
Michard, A., Albarède, F., 1986. The REE content of some hydrothermal fluids. Chem. Geol. 55, 51–60.
Middelburg, J.J., Nan der Weijden, C.H., Woittiez, J.R., 1988. Chemical processes affecting the mobility of major, minor and trace elements during weathering of granitic rocks. Chem. Geol. 68, 253–273.
Min, M., Chen, J., Wang, J., Wei, G., Fayek, M., 2005. Mineral paragenesis and textures associated with sandstone-hosted roll-front uranium deposits. NW China. Ore Geol. Rev. 26, 51–69.
Mirza, T.A., Karim, K.H., Ridha, S.M., Fatah, C.M., 2021. Major, trace, rare earth element, and stable isotope analyses of the Triassic carbonates along the northeastern Arabian Plate margin: a key to understanding paleotectonics and paleoenvironment of the Avroman (Biston) limestone formation from Kurdistan region, northeastern Iraq. Carbonates Evaporites 36, 1–22.
Mücke, A., Badejoko, T., Akande, S., 1999. Petrographic-microchemical studies and origin of the Agbaja Phanerozoic Ironstone Formation, Nupe Basin, Nigeria: a product of a ferruginized ooidal kaolin precursor not identical to the Minette-type. Miner. Depos. 34 (3), 284–296.
Mukherjee, K., Dutta, N., Chandra, D., Pandalai, H., Singh, M., 1988. A statistical approach to the study of the distribution of trace elements and their organic/inorganic affinity in Lower Gondwana coals of India. Int. J. Coal Geol. 10, 99–108.
Mukhopadhyay, P., Goodarzi, F., Crandlemire, A., Gillis, K., MacNeil, D., Smith, W., 1998. Comparison of coal composition and elemental distribution in selected seams of the Sydney and Stellarton Basins, Nova Scotia, Eastern Canada. Int. J. Coal Geol. 37, 113–141.
Munksgaard, N.C., Lim, K., Parry, D.L., 2003. Rare earth elements as provenance indicators in North Australian estuarine and coastal marine sediments. Estuar. Coast. Shelf Sci. 57, 399–409.
Murray, R.W., Buchholtz ten Brink, M.R., Jones, D.L., Gerlach, D.C., Russ III, G.P., 1990. Rare earth elements as indicators of different marine depositional environments in chert and shale. Geology 18, 268–271.
Nagarajan, R., Armstrong-Altrin, J.S., Kessler, F.L., Hidalgo-Moral, E.L., Dodge-Wan, D., Taib, N.I., 2015. Provenance and tectonic setting of Miocene siliciclastic sediments, Sibuti Formation, northwestern Borneo. Arab. J. Geosci. 8, 8549–8565.
Ning, S., Huang, S., Liu, K., Qin, G., Zhou, Y., Zhang, L., Fan, Y., Guo, A., Yuan, J., 2022. Comparison of genesis of abnormal enrichment of metals in coal between the northern and southern margins of Ordos Basin. J. China Coal Soc. 47 (in Chinese with English abstract).
Ojo, G., Igbokwe, U., Egbuachor, C., Nwozor, K., 2017. Geo-technical properties and geochemical composition of kaolin deposits in parts of Ifon, Southwestern Nigeria. Am. J. Eng. Res. 6, 15–24.
Piper, D.Z., 1974. Rare earth elements in the sedimentary cycle: a summary. Chem. Geol. 14, 285–304.
Qi, H., Hu, R., Zhang, Q., 2007. Concentration and distribution of trace elements in lignite from the Shengli Coalfield, Inner Mongolia, China: Implications on origin of the associated Wulantuga germanium Deposit. Int. J. Coal Geol. 71, 129–152.
Querol, X., Whateley, M., Fernandez-Turiel, J., Tuncali, E., 1997. Geological controls on the mineralogy and geochemistry of the Beypazari lignite, central Anatolia. Turkey. Int. J. Coal Geol. 33, 255–271.
Raðenoviæ, A., 2006. Inorganic constituents in coal. Kem. Ind. 55, 65–71.
Schatzel, S.J., Stewart, B.W., 2003. Rare earth element sources and modification in the Lower Kittanning coal bed, Pennsylvania: implications for the origin of coal mineral matter and rare earth element exposure in underground mines. Int. J. Coal Geol. 54, 223–251.
Senior, C., Granite, E., Linak, W., Seames, W., 2020. Chemistry of trace inorganic elements in coal combustion systems: a century of discovery. Energy Fuels 34, 15141–15168.
Seredin, V.V., Dai, S., 2012. Coal deposits as potential alternative sources for lanthanides and yttrium. Int. J. Coal Geol. 94, 67–93.
Shao, L., Zhang, P., Hilton, J., Gayer, R., Wang, Y., Zhao, C., Luo, Z., 2003. Paleoenvironments and paleogeography of the Lower and lower Middle Jurassic coal measures in the Turpan-Hami oil-prone coal basin, northwestern China. AAPG Bull. 87, 335–355.
Shields, G., Stille, P., 2001. Diagenetic constraints on the use of cerium anomalies as palaeoseawater redox proxies: an isotopic and REE study of Cambrian phosphorites. Chem. Geol. 175, 29–48.
Singh, P., Rajamani, V., 2001. REE geochemistry of recent clastic sediments from the Kaveri floodplains, southern India: implication to source area weathering and sedimentary processes. Geochim. Cosmochim. Acta 65, 3093–3108.
Šmuc, N.R., Dolenec, T., Serafimovski, T., Dolenec, M., Vrhovnik, P., 2012. Geochemical characteristics of rare earth elements (REEs) in the paddy soil and rice (*Oryza sativa* L.) system of Kočani Field, Republic of Macedonia. Geoderma 183, 1–11.
Spears, D., Zheng, Y., 1999. Geochemistry and origin of elements in some UK coals. Int. J. Coal Geol. 38, 161–179.
Sun, Y., Zhao, C., Qin, S., Xiao, L., Li, Z., Lin, M., 2016. Occurrence of some valuable elements in the unique 'high-aluminiumcoals'from the Jungar coalfield, China. Ore Geol. Rev. 72, 659–668.
Tanner, L.H., Wang, X., Morabito, A.C., 2012. Fossil charcoal from the Middle Jurassic of the Ordos Basin, China and its paleoatmospheric implications. Geoscience 3, 493–502.
Tatar, A., Alipour-Asll, M., 2020. Geochemistry of major, trace and rare earth elements in coals from the Tazareh mine, eastern Alborz coalfield, NE Iran. Geochem-Explor. Environ. A 20, 381–398.
Taylor, S.R., McLennan, S., 1981. The composition and evolution of the continental crust: rare earth element evidence from sedimentary rocks. Philosophical Transactions of the Royal Society of London. Series A. Math. Phys. Sci. 301, 381–399.
Taylor, S.R., McLennan, S.M., 1985. The Continental Crust: Its Composition and Evolution. Blackwell Scientific Publications.
Trueman, C.N., Tuross, N., 2002. Trace elements in recent and fossil bone apatite. Rev. Mineral. Geochem. 48, 489–521.
USGS (United States Geological Survey)., 2021. Mineral Commodity Summaries. US Geological Survey (Reston, VA), 200 pp.
Van der Weijden, C., Van der Weijden, R.D., 1995. Mobility of major, minor and some redox-sensitive trace elements and rare-earth elements during weathering of four granitoids in central Portugal. Chem. Geol. 125, 149–167.
Vassilev, S.V., Vassileva, C.G., 2007. A new approach for the classification of coal fly ashes based on their origin, composition, properties, and behaviour. Fuel 86, 1490–1512.
Wang, S., 1996. Coal accumulating and coal resource evaluation of Ordos Basin. China Coal Industry Publishing House (Beijing), p. 437 pp..
Wang, X., Jiao, Y., Wu, L., Rong, H., Wang, X., Song, J., 2014. Rare earth element geochemistry and fractionation in Jurassic coal from Dongsheng-Shenmu area, Ordos Basin. Fuel 136, 233–239.
Wang, L., Lv, D., Hower, J.C., Zhang, Z., Raji, M., Tang, J., Liu, Y., Gao, J., 2022. Geochemical characteristics and paleoclimate implication of Middle Jurassic coal in the Ordos Basin, China. Ore Geol. Rev. 144, 104848.
Wang, D., Shao, L., Li, Z., Li, Z., 2012. Palaeogeographic characteristics of the Middle Jurassic Yan'an Age in northern Shaanxi Province. J. Palaeogeo-English 14, 451–460.
Wang, X., Wang, X., Pan, S., Yang, Q., Hou, S., Jiao, Y., Zhang, W., 2018. Occurrence of analcime in the middle Jurassic coal from the Dongsheng Coalfield, northeastern Ordos Basin, China. Int. J. Coal Geol. 196, 126–138.
Wronkiewicz, D.J., Condie, K.C., 1987. Geochemistry of Archean shales from the Witwatersrand Supergroup, South Africa: source-area weathering and provenance. Geochim. Cosmochim. Acta 51, 2401–2416.
Wu, K., Liu, S., Kandasamy, S., Jin, A., Lou, Z., Li, J., Wu, B., Wang, X., Mohamed, C.A., Shi, X., 2019. Grain-size effect on rare earth elements in Pahang River and Kelantan River, Peninsular Malaysia: Implications for sediment provenance in the southern South China Sea. Cont. Shelf. Res. 189, 103977.
Xu, M., Yan, R., Zheng, C., Qiao, Y., Han, J., Sheng, C., 2004. Status of trace element emission in a coal combustion process: a review. Fuel Process. Technol. 85, 215–237.
Yan, X., Dai, S., Graham, I.T., French, D., Hower, J.C., 2019. Mineralogy and geochemistry of the Palaeogene low-rank coal from the Baise Coalfield, Guangxi Province, China. Int. J. Coal Geol. 214, 103282.
Yossifova, M.G., Eskenazy, G.M., Valčeva, S.P., 2011. Petrology, mineralogy, and geochemistry of submarine coals and petrified forest in the Sozopol Bay, Bulgaria. Int. J. Coal Geol. 87, 212–225.
Zhang, H., Li, H., Xiong, C., Zhang, H., Wang, Y., He, Z., Lin, G. Sun, B., 1998. Jurassic coal-bearing strata and coal accumulation in northwestern China: Beijing, China, Geological Publishing House, 249-251 pp.
Zhang, J., Ren, D., Zhu, Y., Chou, C.-L., Zeng, R., Zheng, B., 2004. Mineral matter and potentially hazardous trace elements in coals from Qianxi Fault Depression Area in southwestern Guizhou, China. Int. J. Coal Geol. 57, 49–61.
Zhang, Z., Lv, D., Wang, C., Hower, J.C., Raji, M., Wang, T., Zhang, J., Yang, Y., 2022. Mineralogical and geochemical characteristics of tonsteins from the Middle Jurassic Yan'an Formation, Ordos Basin, North China. Int. J. Coal Geol. 253, 103968.
Zhang, Z., Wang, T., Ramezani, J., Lv, D., Wang, C., 2021. Climate forcing of terrestrial carbon sink during the Middle Jurassic greenhouse climate: Chronostratigraphic analysis of the Yan'an Formation, Ordos Basin, North China. GSA Bull. 133, 1723–1733.

Zhang, X., Zhang, F., Xin, C., Zhang, W., Han, D., 2012. REEs fractionation and sedimentary implication in surface sediments from eastern South China Sea. J. Rare Earth 30, 614–620 (in Chinese with English abstract).
Zhao, L., Dai, S., Nechaev, V.P., Nechaeva, E.V., Graham, I.T., French, D., Sun, J., 2019. Enrichment of critical elements (Nb-Ta-Zr-Hf-REE) within coal and host rocks from the Datanhao mine, Daqingshan Coalfield, northern China. Ore Geol. Rev. 111, 102951.
Zhao, C., Duan, D., Li, Y., Zhang, J., 2012. Rare earth elements in No. 2 coal of Huangling mine, Huanglong coalfield. China. Energy Explor. Exploit. 30, 803–818.